TECTONO-MAGMATIC SETTING OF THE JURASSIC OPHIOLITES FROM THE SOUTH APUSENI MOUNTAINS (ROMANIA): PETROLOGICAL AND GEOCHEMICAL EVIDENCE

Emilio Saccani*, Ionel Nicolae** and **Renzo Tassinari***

***** *Dipartimento di Scienze della Terra, Università di Ferrara, 44100 Ferrara, Italy (e-mail: sac@dns.unife.it)*
****** *Institutul Geologic al Romaniei, 79678 Bucuresti, Romania*

Keywords: *ophiolites, MORB, petrology, geochemistry, Jurassic. South Apuseni Mountains, Romania.*

ABSTRACT

In the South Apuseni Mountains (Romania), Jurassic ophiolites can be found in association with Upper Jurassic - Lower Cretaceous island-arc magmatic suites, within a narrow belt which marks the boundary between the Eurasian and Apulian Palaeozoic continental margins. These ophiolites are highly dismembered, and sections of the lowermost crust and upper mantle are not present. New data on the field occurrence, petrology, and geochemistry of the plutonic, subvolcanic, and volcanic ophiolitic units are presented. The plutonic rocks consist of both layered and isotropic gabbros, as well as subordinate Fe-gabbros, and quartz-diorites. Ultramafic cumulates are very scarce, and include plagioclase-dunites and plagioclase-wehrlites. The subvolcanic section is represented by typical sheeted dyke complexes, cropping out in several localities and including basalts and basaltic andesites. The volcanic section includes pillowed and massive lava flows, as well as subordinate volcanic breccias, all displaying high-Ti magmatic affinity. The geochemical characteristics of these volcanic rocks are very similar to those of basalts generated at Mid-Ocean Ridge (MORBs), as well as those of the high-Ti ophiolitic complexes of the Dinaride and Hellenide orogenic belts. The constituent minerals of the intrusives are olivine, plagioclase, clinopyroxene (rarely orthopyroxene), Cr-spinel, and Fe-Ti-oxides. The subvolcanic and volcanic rocks contain plagioclase, clinopyroxene, and Fe-Ti oxides. The clinopyroxene chemistry also confirms the high-Ti affinity.

INTRODUCTION

In the South Apuseni Mountains (SAM), different Jurassic - Lower Cretaceous magmatic suites are distributed along a narrow belt, which marks the border between the Eurasian plate and the Tisza (AustroBihorean) microplate (Sandulescu, 1984), the latter probably belonging to the northernmost edge of the Apulian plate (Dal Piaz et al., 1995; Dallmeyer et al., 1999).

Principally on the basis of their present tectonic setting, these ophiolites, though composite, have been described by many authors as a single ophiolitic belt, although different interpretations of the geodynamic significance of the individual magmatic suites have been proposed (e.g. Savu, 1980; Cioflica et al., 1980; 1981; Cioflica and Nicolae, 1981). However, recent studies on the field relations, petrology and geochemistry of the various rock types from the SAM Jurassic - Lower Cretaceous magmatic associations (Savu, 1996; Bortolotti et al., 1999) suggest that two distinct petro-structural units are present: a Jurassic ophiolitic unit, and an Upper Jurassic - Lower Cretaceous island arc magmatic association. In particular, ophiolites are stratigraphically overlain by an island arc magmatic sequence which includes members of the medium-K and high-K calc-alkaline magmatic series (Nicolae and Saccani, in prep.), in turn capped by Upper Jurassic - Lower Cretaceous carbonates. In addition, calc-alkaline plutonic rocks intrude the ophiolitic sequence (Savu et al., 1996), suggesting that island arc magmatic activity took place while the ophiolitic sequence was at least partially structurally emplaced.

The magmatic affinity and petrogenetic significance of the SAM ophiolitic suite are still under debate. Two main interpretations are currently accepted: (1) the ophiolites are fragments of a Jurassic MORB-type oceanic crust (Savu et al., 1981; Savu et al., 1994a); and (2) ophiolites are fragments of a Jurassic arc-type oceanic crust representing the first stage of an intra-oceanic arc whose development subsequently led to the production of calc-alkaline magmatism (Cioflica et al., 1980; Cioflica and Nicolae, 1981; Nicolae, 1995).

This study presents new data on the petrology and rock chemistry of the ophiolitic sequences exposed in the SAM (Fig. 1) with the purpose of constraining their compositions, defining their magmatic evolution, and assessing their tectono-magmatic formation environment. The composition, petrogenesis, and evolution of the island arc magmatic suites will be discussed elsewhere (Nicolae and Saccani, in prep.).

BASIC GEOLOGICAL SETTING

The Apuseni Mountains represent a narrow structural belt located in the innermost part of the Carpathian orogenic belt (Fig. 1). They can be tectonically subdivided in two main zones: the North Apuseni and South Apuseni Mountains. The first zone (also known as Internal Dacides) includes several nappe complexes (Sandulescu, 1984), all consisting of a polydeformed, “Austroalpine-type” crystalline basement covered by Permian-Lower Cretaceous sedimentary sequences.

By contrast, the South Apuseni Mts. (SAM) are characterized by the presence of the most widespread ophiolitic sequence of the Carpathians (Fig. 1). Their structure is made up by a pile of tectonic units known as the Mureş Nappe complex (Bortolotti et al., 1999). The Mureş Nappe complex marks the boundary separating the Paleozoic rocks of the ancient continental margin of the Eurasian plate, to the north, from the Tisza (AustroBihorean) microplate, to the south (Kovacs, 1982; Sandulescu, 1984), possibly representing the northernmost edge of the Apulian plate, to the south (Dal Piaz et al., 1995; Dalmeyer et al., 1999). To the south, the Mureş Nappe complex is separated from the Bucovino-Getic Nappes of the South Carpathians (Marginal Dacides) by the Miocene south-Transylvanian fault-system, for which

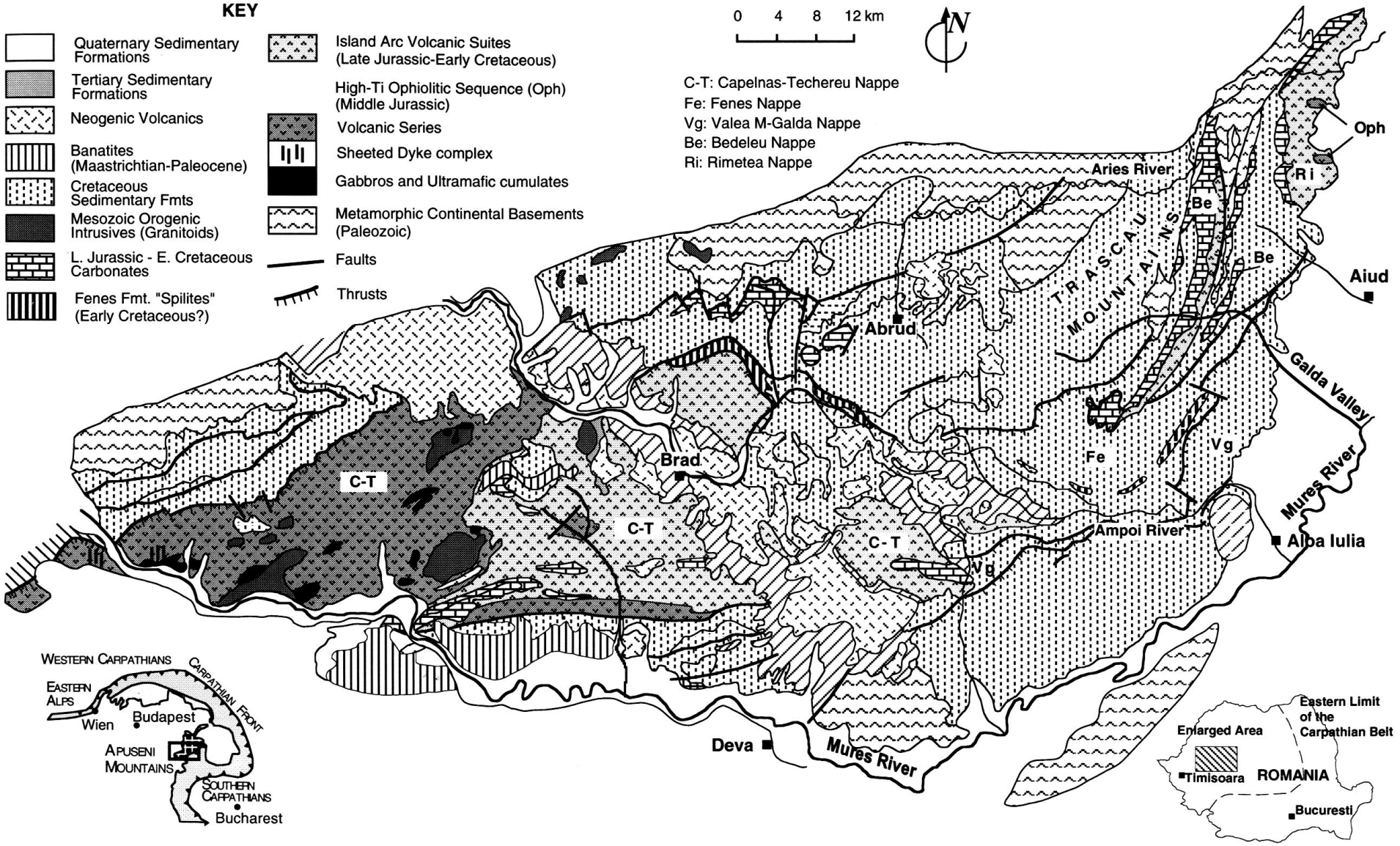

Fig. 1 - Simplified geological sketch-map of the South Apuseni Mountains (modified after Cioflica et al., 1981 and Nicolae, 1985). Location of the study area, as well as the position of the South Apuseni Mountains with respect to the Carpathian Belt, are also shown.

a dextral transpression of about 300 km has been postulated (Burchfiel, 1980).

Ophiolites (Fig. 1) crop out extensively in the central part of SAM (Capalnas-Techereu Nappe), and subordinately in the Trascau Mountains (Feneş and Rimetea Nappes). In both cases they are always overlain by Upper Jurassic - Lower Cretaceous island arc volcanic rocks (Cioflica and Nicolae, 1981; Savu et al., 1981; Savu, 1990) and are intruded by Lower Cretaceous calc-alkaline granitoids (Savu et al., 1996). The ophiolitic sequence includes rock types representing the upper part of the oceanic crust, comprising very scarce ultramafic cumulates, small gabbroic bodies, a well-developed sheeted dyke complex and a volcanic sequence. Locally, radiolarian cherts, Callovian to Oxfordian in age, are found at the top of the basaltic sequence (Lupu et al., 1995).

The interpretation of the tectono-magmatic significance of the SAM ophiolites, as well as of their relationships with the island arc magmatic series, is still under debate. On one hand, the ophiolites are interpreted as fragments of a Jurassic oceanic crust generated at a mid-ocean ridge. In this model, they were emplaced in their present position starting in the Late Jurassic, as a result of the closing of the oceanic basin (Mureş Ocean) within which the SAM ophiolites were formed (Savu et al., 1994a; Savu et al., 1994b), and there are no genetic relationships between the ophiolites and the overlying island arc rocks (Savu et al., 1981). On the other hand, this interpretation requires spatial and temporal genetic relationships between the ophiolites and the island arc series. In particular, the ophiolites are interpreted by Cioflica et al. (1980), Cioflica and Nicolae (1981), and Nicolae, (1995) as fragments of an arc-type oceanic crust generated in an intra-oceanic arc whose development subsequently led to the production of the island arc magmatism. In this hypothesis, a petrological and geochemical evolution from ophiolitic MORB to overlaying island arc lavas is assumed (Cioflica and Nicolae, 1981).

The age of the ophiolitic sequence is still uncertain. Several K/Ar dates on basaltic rocks have been obtained by Nicolae et al. (1992), and show a wide range of variation from 138.9±6 to 167.8±5 Ma. Such puzzling disparities in age probably reflect perturbations associated with the intrusion of calc-alkaline dykes. However, the oldest age of 167.8±5 Ma can be assumed as the closest age for the ophiolitic sequence, as also confirmed by the Callovian to Oxfordian radiolarian ages. Moreover, the 155 Ma age of the calc-alkaline intrusions (Pana, 1998), as well as the Oxfordian to lowermost Tithonian age of limestones intercalated in the upper part of the island arc volcanic sequence, confirm this assumption. In summary, these data suggest a Middle Jurassic age for the ophiolitic sequence.

FIELD OCCURRENCE

The SAM ophiolitic complex is characterized by a prevalence of volcanic rocks over mafic intrusives. Ultramafic mantle tectonites are lacking, while ultramafic cumulates are very scarce and restricted to a few parts of some of the gabbroic intrusions. In general, the most complete ophiolitic sequences of SAM are found in the Capalnas-Techereu nappe (C-T), while there are very small outcrops of ophiolitic volcanics in the Feneş and Rimetea Nappes (Fig. 1). Although tectonically dismembered, the ophiolitic sequence (Fig. 2) can reasonably be interpreted as composed of (from bottom to top): (1) ultramafic-mafic cumulates, (2) isotropic gabbros and diorites, (3) sheeted dyke complex, (4) volcanic sequence, and (5) very scarce Callovian - Oxfordian radiolarian cherts (Nicolae et al., 1992).

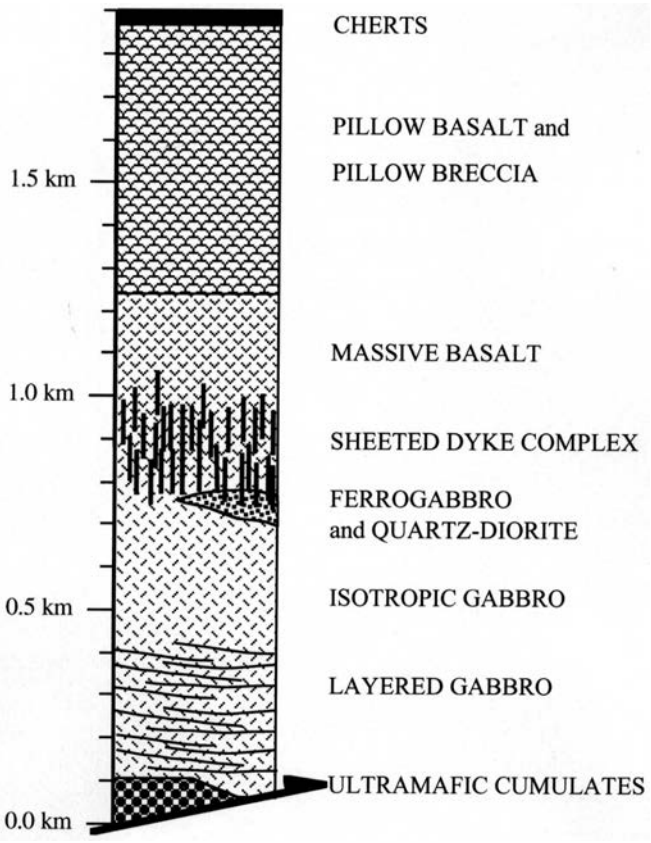

Fig. 2 - Schematic stratigraphical column of the SAM ophiolitic sequence.

Intrusives are represented by a series of small, discontinuous bodies scattered throughout the C-T Nappe (Fig. 1). These bodies include very scarce ultramafic cumulates, melagabbros, gabbros and rare gabbronorites associated with ferrogabbros and quartz-diorites. Ultramafic cumulates are the lowest preserved pseudostratigraphic unit in the SAM ophiolites, and include alternations of plagioclase-wehrlites and plagioclase-dunites, depending on the amount of modal clinopyroxene. Gabbros show both layered and isostropic textures; compositional layering is dominantly centimeter-to-decameter scale, and is defined by modal variations of primary plagioclase and clinopyroxene. The overlying sheeted dyke complex is well developed in the southwestern part of the C-T Nappe and, subordinately, in the Feneş Nappe (Fig. 1). Previous studies (e.g. Savu et al.,1994a) indicate a much greater occurrence of sheeted dykes in the C-T nappe, although detailed field work, cast doubt on this inference. Dykes have rather uniform widths, ranging from 20 to 30 cm, and contain characteristic one-way few centimetres-wide chills. The transition from the sheeted dykes into the volcanic sequence is poorly-exposed; only in few localities can a sharp transition (over a thickness of approximately 100 meters) be observed. The volcanic sequence is dominated by basaltic pillow and massive lava flows. Moreover, pillow breccias, sometimes associated with arenites, can locally be found between the different lava flows. Pillows are generally less than one meter in diameter, while massive flows are 1-5 m thick. The pillows orientations indicate that dips are deep to vertical. A few me-

ters of radiolarian cherts overly the basaltic sequence in a few places. Individual 0.3-1 m thick dolerite dykes are very common. Both the intrusive and extrusive sequences are locally cut by dolerite dykes showing vary variable sizes (from few centimetres to more than 1 metre).

In C-T, Feneş and Rimetea nappes, ophiolites are overlain by island arc rocks of the medium-K and high-K calc-alkaline series (Nicolae and Saccani, in prep.). Moreover, calc-alkaline dykes ranging in composition from andesites to dacites and rhyolites are widespread at all levels throughout the ophiolitic sequence. In addition, some granitoid intrusions showing calc-alkaline affinity are located in the western areas of the C-T Nappe (Fig. 1); these mainly consist of granites and granodiorites, though diorites are locally found at the marginal zones of the intrusions (Savu et al., 1996).

SAMPLING AND METHODS

The samples analyzed in this paper represent extensive geographical and stratigraphical coverage of the various ophiolitic rock types cropping out in the C-T, Feneş and Rimetea Nappes (Fig. 1). A total of 130 samples was collected and analyzed.

The electron microprobe analyses were performed at the University of Florence using a JEOL-JXA 8600 automated microanalyser. The operating conditions were: sample current of 10 nA and accelerating potential of 15 KV. Counting time was 100 seconds for peak and 20 sec for background positions. Results are presented in Tables 1-4.

Bulk rock major and 10 trace element analyses were determined on pressed powder pellets using an automated Philips PW1400 X-ray fluorescence (XRF) spectrometer at the Institute of Mineralogy of the University of Ferrara. Matrix correction methods proposed by Franzini et al. (1975) and Leoni and Saitta (1976) were applied. Replicate analyses were made on trace elements, indicating a precision ranging from ±1% to ±2%. Representative chemical compositions are given in Table 5.

Volatiles were determined as loss on ignition (L.O.I.) at 1000°C. Because, a considerable number of the studied samples contained calcite veins, CO_2 content was also determined by simple volumetric technique (Jackson, 1958). The precision of the CO_2 measurement was checked by analyzing 20 reference samples with different CO_2 contents. The mean absolute percentage error and the detection limit were, respectively, 3% and 0.5%.

Rare Earth Elements (REE), Sc, Nb, Hf, Ta, Th, and U (Table 6) were determined by Inductively Coupled Plasma-Mass spectrometry (ICP-MS) at the Institute of Mineralogy, University of Ferrara, using a VG Elemental Plasma Quad PQ2 Plus. Accuracy and detection limits were calculated by analyzing a set of international standards, including: JP-1, JGb-1, BHVO-1, UB-N, BE-N, BR, GSR-3, and AN-G. Detection limits (in ppm) are: Sc = 0.29; Y, Nb, Hf, Ta = 0.02; REE <0.14; Th, U = 0.011. The accuracy for analyzed elements is in the range of 0.9-7.9 relative %, with the exception of Gd (10.2 relative %).

MINERAL CHEMISTRY

Olivine

Olivine is an early cumulus phase in the ultramafic cumulates and olivine-gabbros, accounting for up to 10-15% of the mode as small rounded crystals poikilitically enclosed in clinopyroxene. Olivine usually underwent early serpentinization, which is assumed to have taken place in the oceanic environment at low temperature. Fresh olivine relics are found in a few plagioclase-bearing wehrlites. As shown in Table 1, they are chemically homogeneous and unzoned, their Fo-contents ranging from 80 to 82. NiO contents range from 0.16wt% to 0.23wt%, while Cr_2O_3 is always less than 0.05wt%. There is no correlation between NiO or Cr_2O_3 and Fo-content.

Table 1 - Representative microprobe analyses of olivine from the SAM plagioclase-wehrlite (Pl-Wr).

Locality	Marcului	Marcului	Marcului
Sample	AP114	AP114	AP114
Rock	Pl-Wr	Pl-Wr	Pl-Wr
Mineral	Ol1-1	Ol1-2	Ol2-1
SiO_2	39.85	39.68	39.29
TiO_2	0.00	0.01	0.07
Al_2O_3	0.00	0.05	0.07
Cr_2O_3	0.00	0.05	0.01
Fe_2O_3	0.00	0.00	0.00
FeO	16.78	16.29	18.12
MnO	0.27	0.20	0.25
MgO	43.75	43.71	42.41
CaO	0.17	0.20	0.10
NiO	0.21	0.16	0.23
Oxide total	101.03	100.35	100.55
Si	0.999	0.999	0.997
Ti	0.000	0.000	0.001
Al	0.000	0.001	0.002
Cr	0.000	0.001	0.000
Fe^{3+}	0.000	0.000	0.000
Fe^{2+}	0.352	0.343	0.384
Mn	0.006	0.004	0.005
Mg	1.635	1.641	1.603
Ca	0.005	0.005	0.003
Ni	0.004	0.003	0.005
Cation total	3.001	2.999	3.001
Mg#	82.3	82.7	80.7
Forsterite	82.1	82.5	80.4
Fayalite	17.7	17.3	19.3
Tephroite	0.3	0.2	0.3

Mg# = 100*Mg/(Mg+Fe). Atomic proportions are calculated on 4 oxigens.

Plagioclase

In all rock types, plagioclase has experienced varying degrees of ocean-floor hydrothermal alteration, resulting in the replacement of primary crystals with albite ± calcite or prehnite. In this work, only fresh crystals were selected for analyses. Plagioclase is a cumulus phase in the ultramafic and mafic cumulates, where it forms tabular crystals enclosed in poikilitic clinopyroxene. Its composition is moderately calcic, and covers a wide range of variation, from An_{40} to An_{80} (Table 2, Fig. 3). More calcic compositions are found in isotropic gabbros (An_{52-88}), while diorites contain less calcic plagioclase (An_{25-48}). Plagioclase from sheeted dykes is commonly found in fresh rocks as fine-grained tabular crystals forming an intersertal texture with clinopyroxene, and shows compositions comparable to those of isotropic gabbros (An_{50-85}). Although usually scarce (<15%), plagioclase (An_{45-78}) is the dominant phenocryst phase in individual dolerite dykes and volcanic rocks, exhibiting considerable zoning (Fig. 3). There are no compositional variations between core and rim or between phenocrysts and groundmass minerals in the same sample. This could be explained by the continuous supply of primitive melts to the magma chamber.

Table 2 - Selected microprobe analyses of plagioclase from the SAM ophiolites.

	Intrusive Sequence							Sheeted Dyke Complex					Volcanic and Subvolcanic Sequence			
Locality	Marcului	Julita	Cuias	V.Rosiuta	V.Rosiuta	A-Saliste	A-Saliste	Julita	Lalasint	Lalasint	Lalasint	Lalasint	Tataroaia	Tataroaia	Tataroaia	Ponor
Sample	AP114	AP129	AP144B	AP108	AP108	AP11	AP11	AP123C	AP134	AP134	AP134	AP134	AP164	AP164	AP164	AP25
Rock	Pl-Wr	Gb	Gb	Gb	Gb	Di	Di	HT-B	HT-B	HT-B	HT-B	HT-B	HT-B	HT-B	HT-B	HT-B
Note													Pillow	Pillow	Pillow	Dy
Mineral	Pl3-2	Pl1-1	Pl3-1	Pl3-2	Pl3-3c	Pl4-3c	Pl4-3r	Pl1-1	Pl1-2	Pl2-1c	Pl2-1r	Pl6-1 (g)	Pl2-1	Pl3-1	Pl3-2	Pl6-2
SiO_2	48.39	51.10	47.37	54.56	51.39	60.68	56.99	48.92	47.89	52.37	52.84	53.43	53.09	52.24	52.89	56.99
TiO_2	0.05	0.06	0.03	0.04	0.06	0.01	0.00	0.06	0.06	0.05	0.09	0.16	0.06	0.04	0.03	0.01
Al_2O_3	32.41	31.35	33.97	28.98	31.19	25.22	27.76	32.38	33.20	30.09	30.03	28.93	29.64	29.20	29.84	26.91
Cr_2O_3	0.05	0.00	0.00	0.00	0.00	0.00	0.02	0.04	0.00	0.02	0.00	0.00	0.04	0.02	0.00	0.00
Fe_2O_3	0.00	0.00	0.00	0.00	0.00	0.00	0.00	0.00	0.00	0.00	0.00	0.00	0.00	0.00	0.00	0.00
FeO	0.63	0.72	0.37	0.70	0.59	0.23	0.20	0.39	0.42	0.61	0.61	0.91	0.92	0.90	0.88	0.62
MnO	0.00	0.03	0.06	0.05	0.04	0.00	0.00	0.05	0.00	0.00	0.00	0.02	0.00	0.00	0.03	0.00
MgO	0.18	0.16	0.02	0.07	0.19	0.07	0.02	0.28	0.16	0.19	0.18	0.20	0.24	0.14	0.23	0.08
CaO	15.54	13.57	16.12	11.67	14.48	6.39	8.93	15.15	17.02	13.58	12.88	12.16	12.80	12.57	13.15	9.42
Na_2O	2.30	3.55	2.05	4.75	3.39	7.45	5.94	2.42	1.82	3.80	4.07	4.29	4.05	4.37	3.85	6.30
K_2O	0.01	0.04	0.03	0.08	0.06	0.51	0.21	0.04	0.02	0.05	0.05	0.05	0.03	0.04	0.02	0.09
Total	99.56	100.58	100.02	100.90	101.39	100.56	100.07	99.73	100.59	100.76	100.75	100.15	100.87	99.52	100.92	100.42
Si	2.226	2.315	2.171	2.448	2.314	2.687	2.551	2.241	2.187	2.366	2.382	2.421	2.393	2.390	2.383	2.554
Ti	0.002	0.002	0.001	0.001	0.002	0.000	0.000	0.002	0.002	0.002	0.003	0.005	0.002	0.001	0.001	0.000
Al	1.758	1.674	1.836	1.533	1.656	1.317	1.465	1.749	1.787	1.602	1.596	1.545	1.575	1.575	1.585	1.422
Cr	0.002	0.000	0.000	0.000	0.000	0.000	0.001	0.001	0.000	0.001	0.000	0.000	0.001	0.001	0.000	0.000
Fe^{3+}	0.000	0.000	0.000	0.000	0.000	0.000	0.000	0.000	0.000	0.000	0.000	0.000	0.000	0.000	0.000	0.000
Fe^{2+}	0.024	0.027	0.014	0.026	0.022	0.009	0.007	0.015	0.016	0.023	0.023	0.034	0.035	0.034	0.033	0.023
Mn	0.000	0.001	0.002	0.002	0.002	0.000	0.000	0.002	0.000	0.000	0.000	0.001	0.000	0.000	0.001	0.000
Mg	0.012	0.011	0.001	0.005	0.013	0.005	0.001	0.019	0.011	0.013	0.012	0.014	0.016	0.010	0.015	0.005
Ca	0.766	0.659	0.792	0.561	0.699	0.303	0.428	0.744	0.833	0.657	0.622	0.590	0.618	0.616	0.635	0.452
Na	0.205	0.312	0.182	0.413	0.296	0.640	0.515	0.215	0.161	0.333	0.356	0.377	0.354	0.388	0.336	0.548
K	0.001	0.002	0.002	0.005	0.003	0.029	0.012	0.002	0.001	0.003	0.003	0.003	0.002	0.002	0.001	0.005
Cation total	4.995	5.003	5.002	4.99	5.01	4.989	4.980	4.99	5.00	5.00	5.00	4.99	5.00	5.02	4.99	5.011
Albite	20.4	30.8	18.3	40.9	28.6	30.8	44.4	21.6	15.8	32.4	35.0	37.0	34.5	36.9	32.9	43.8
Anorthite	76.0	65.1	79.7	55.5	67.5	65.0	53.4	74.6	81.5	63.9	61.2	57.9	60.3	58.7	62.1	53.0
Orthoclase	0.1	0.2	0.2	0.5	0.3	2.9	1.2	0.2	0.1	0.3	0.3	0.3	0.2	0.2	0.1	0.5

Pl-Wr- plagioclase-wehrlite; Gb- gabbro; Di- diorite; Dy- individual dyke; HT-B- high-Ti basalt; c- core; r- rim; (g)- groundmass. Atomic proportions are calculated on 8 oxigens.

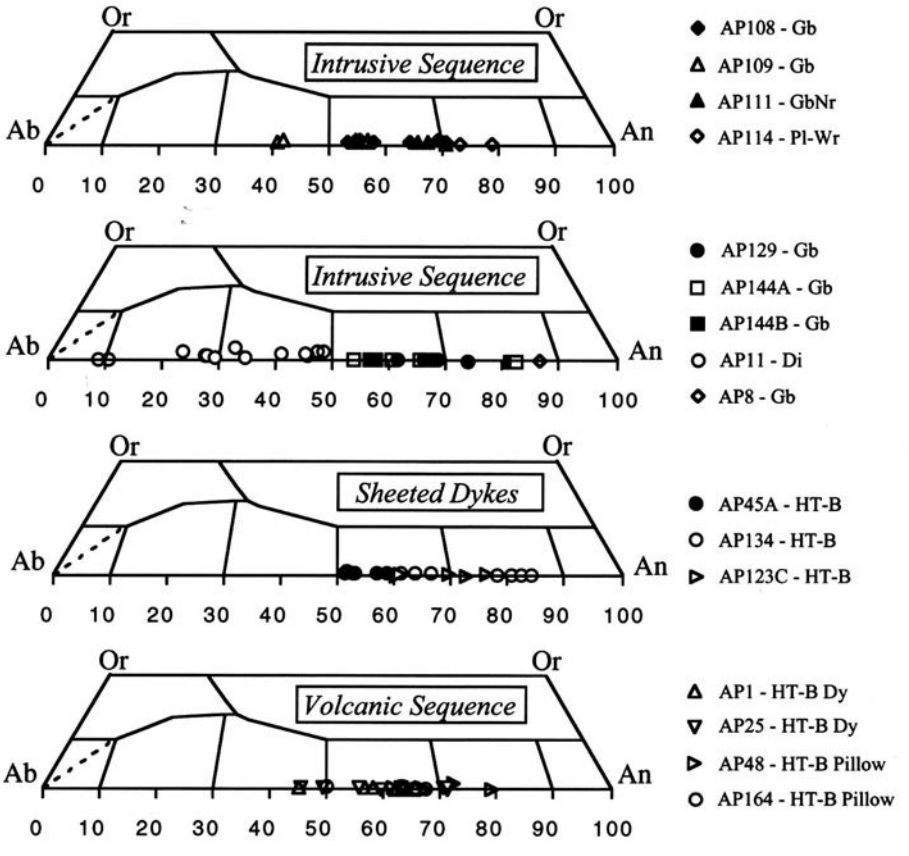

Fig. 3 - Compositions of plagioclase from the SAM ophiolites. Gb- gabbro; GbNr- gabbronorite; Pl-Wr- plagioclase wehrlite; Di- diorite; Dy- individual dyke; P- pillow; HT-B- high-Ti basalt.

Pyroxenes

Primary pyroxene crystals are scarce in all rock types, as they are usually replaced by Fe-actinolite during ocean-floor metamorphism. Chemical data on preserved crystals are presented in Table 3. Adcumulus clinopyroxene in plagioclase-bearing ultramafic rocks (<8% of the mode) is commonly coarse-grained and poikilitic, while in gabbros (~30% of the mode) it is found as granular either anhedral or interstitial. In both cases, it shows highly uniform chemistry. Compositionally, clinopyroxene is magnesium-rich augite (according to the classification of Morimoto, 1989) in Pl-dunites and Pl-wehrlites, having Mg# [defined as: 100xMg/(Mg+Fe)] of 85.6-90.0, and varies from endiopside to augite in cumulitic gabbros and gabbronorite. Its composition on the pyroxene quadrilateral is shown in Fig. 4. Orthopyroxene (sub-calcic augite) has only been observed as a cumulus phase in the rare gabbronorites. Clinopyroxenes from both isotropic and cumulate gabbros range from diopside to augite, extending into the magnesium-rich augite compositions. The Cr_2O_3 content exhibits a weak positive correlation with Mg# in clinopyroxenes from ultramafites, but not in clinopyroxenes from gabbros, where it is extremely variable (0.00%wt to 0.24wt%). The TiO_2 content is reasonably high (0.41wt% - 0.52wt%, reaching 0.85wt% in few crystal rims), suggesting an origin from high-Ti tholeiitic parental liquids. The Al_2O_3 content of both clinopyroxenes lies between 1.10wt% and 3.18wt% (Fig. 4). Overall, clinopyroxenes have a light rough Fe-enrichment trend.

Clinopyroxenes from subvolcanic and volcanic rocks are usually found as granular microliths in an intersertal groundmass. As observed in Fig. 4, they are very variable in composition, mainly lying in the augite field, but also extending to diopsidic to magnesium-rich augite compositions. They are chemically distinct from clinopyroxenes of intrusive rocks for their higher TiO_2, (0.2wt% - 2.6wt%), Cr_2O_3 (0.0wt% - 0.5wt%), and Al_2O_3 (1.8wt% - 4.1wt%). The Al_2O_3 content of diopsides is considerably high (4.7 wt% to 7.15wt%). Clinopyroxenes have been plotted in the discrimination diagram of Fig. 5 (Beccaluva et al., 1989), where they reveal a close affinity with clinopyroxenes of normal-MORBs.

Chrome Spinels and Fe-Ti oxides

Chrome spinels are accessory phases in plagioclase ultramafic rocks (Table 4). They are euhedral to subhedral, and account for ca. 0.5% (occasionally up to 2%) of the mode. The grain size is always very small (<0.5 mm). Chrome spinels disappear in the overlying cumulate rocks because of the extensive appearance of clinopyroxene, which accommodates the chromium (Dickey et al., 1971).

In the plagioclase dunites, chrome spinels are typically Cr-rich and Al-poor (Cr#, defined as 100*Cr/(Cr+Al) = 58.7-83.5). In plagioclase-wehrlites, Cr_2O_3 content is significantly lower (Cr# = 61.8-65.5). Their composition, however, slightly contrasts with that of chromites from oceanic peridotites. Chromites from oceanic peridotites have Cr# less than 60 (Dick and Bullen, 1984). By contrast, Cr# for studied samples is greater than 61.8. This disparity could be interpreted as the consequence of Cr and Fe partitioning between early cumulate chromite and clinopyroxene.

Fe-Ti oxides are accessory minerals in all intrusive and volcanic rocks. They include titanomagnetite (TiO_2 = 3.71wt% - 26.05wt%) and magnetite (TiO_2 = 0.00wt% -

Table 3 - Selected microprobe analyses of pyroxene from the SAM ophiolites.

	Intrusive Sequence						Sheeted Dyke Complex				Volcanic Sequence		Dykes	
Locality	Sovarului	Sovarului	V. Rosiuta	V. Rosiuta	V. Rosiuta	Julita	Julita	Julita	Lalasint	Lalasint	Batuta	Batuta	Sovarului	Sovarului
Sample	AP3	AP3	AP111	AP111	AP111	AP129	AP45A	AP45A	AP134	AP134	AP137	AP137	AP1	AP1
Rock	Pl-Du	Pl-Du	GbNr	GbNr	GbNr	Gb	HT-B	HT-B	HT-B	HT-B	HT-B	HT-B	HT-B	HT-B
Note											MLF	MLF		
Mineral	Cpx2-1c	Cpx2-1r	Opx1-3	Opx1-4	Cpx3-1	Cpx2-1	Cpx3-1	Cpx3-2	Cpx4-1c	Cpx6-1c	Cpx2-1c	Cpx2-1r	Cpx3-1	Cpx3-2
SiO_2	53.15	52.70	52.60	52.61	52.48	53.12	51.70	51.85	52.75	51.54	53.04	51.53	51.41	50.92
TiO_2	0.37	0.42	0.37	0.45	0.47	0.42	0.71	0.59	0.46	0.49	0.51	0.88	0.78	1.19
Al_2O_3	2.45	2.77	1.02	1.04	1.73	2.32	3.21	2.62	2.85	3.12	2.48	3.22	3.50	3.30
Cr2O3	0.58	0.58	0.00	0.00	0.43	0.21	0.36	0.00	0.57	0.50	0.67	0.18	0.01	0.00
Fe_2O_3	0.00	0.00	0.00	0.00	0.00	0.00	0.00	0.00	0.00	0.00	0.00	0.00	0.00	0.00
FeO	4.61	4.37	22.05	19.30	6.11	6.06	6.66	10.25	4.70	5.58	6.91	8.26	7.19	10.65
MnO	0.03	0.11	0.55	0.46	0.16	0.19	0.12	0.26	0.14	0.15	0.13	0.16	0.21	0.27
MgO	17.68	17.52	21.52	23.13	17.49	17.87	17.00	16.22	17.68	17.50	17.81	16.02	16.12	14.69
CaO	21.09	21.32	1.99	2.02	19.15	19.22	20.16	18.11	20.31	19.42	18.97	18.97	20.10	18.58
Na_2O	0.19	0.27	0.00	0.03	0.30	0.27	0.28	0.30	0.35	0.26	0.25	0.22	0.26	0.33
Oxide total	100.15	100.06	100.10	99.04	98.32	99.68	100.20	100.20	99.81	98.56	100.77	99.44	99.58	99.93
Fe_2O_3*	0.18	0.98	0.31	0.44	0.21	0.09	1.94	1.65	0.56	1.04	0.40	0.00	1.02	0.53
FeO*	4.45	3.49	21.77	18.90	5.92	5.98	4.91	8.77	4.20	4.64	6.55	8.26	6.28	10.17
Total*	100.17	100.16	100.13	99.08	98.34	99.69	100.39	100.37	99.87	98.66	100.81	99.44	99.68	99.98
Si	1.933	1.917	1.963	1.959	1.950	1.944	1.889	1.914	1.923	1.906	1.927	1.911	1.897	1.899
Ti	0.010	0.011	0.010	0.013	0.013	0.012	0.020	0.016	0.013	0.014	0.014	0.025	0.022	0.033
Al	0.105	0.119	0.045	0.046	0.076	0.100	0.138	0.114	0.122	0.136	0.106	0.141	0.152	0.145
Cr	0.017	0.017	0.000	0.000	0.013	0.006	0.010	0.000	0.016	0.015	0.019	0.005	0.000	0.000
Fe^{3+}	0.005	0.027	0.009	0.012	0.006	0.002	0.053	0.046	0.015	0.029	0.011	0.000	0.028	0.015
Fe^{2+}	0.135	0.106	0.679	0.589	0.184	0.183	0.150	0.271	0.128	0.144	0.199	0.256	0.194	0.317
Mn	0.001	0.003	0.017	0.015	0.005	0.006	0.004	0.008	0.004	0.005	0.004	0.005	0.007	0.009
Mg	0.958	0.950	1.197	1.284	0.969	0.975	0.926	0.893	0.960	0.964	0.964	0.886	0.887	0.816
Ca	0.822	0.831	0.080	0.081	0.763	0.754	0.789	0.716	0.793	0.769	0.738	0.754	0.795	0.742
Na	0.013	0.019	0.000	0.002	0.022	0.019	0.020	0.021	0.025	0.019	0.018	0.016	0.019	0.024
Cation total	4.000	4.000	4.000	4.000	4.000	4.000	4.000	4.000	4.00	4.00	4.00	4.00	4.000	4.000
Mg#	87.6	89.9	63.8	68.6	84.0	84.2	86.0	76.7	88.3	87.0	82.9	77.6	82.1	72.0
Other	7.0	9.1	3.7	4.1	5.8	6.4	11.1	9.1	9.0	9.9	7.7	8.9	10.3	10.2
Quad	93.0	90.9	96.3	95.9	94.2	93.6	88.9	90.9	91.1	90.1	92.3	91.2	89.7	89.9
Wollastonite	42.9	44.0	4.1	4.1	39.8	39.4	42.3	38.1	42.2	41.0	38.8	39.8	42.4	39.6
Enstatite	50.0	50.3	61.2	65.7	50.6	51.0	49.6	47.5	51.0	51.4	50.7	46.7	47.3	43.5
Ferrosilite	7.1	5.6	34.7	30.1	9.6	9.6	8.1	14.4	6.8	7.7	10.5	13.5	10.3	16.9

Pl-Du- plagioclase-dunite; GbNr- gabbronorite; MLF- massive lava flow; Cpx- clinopyroxene; Opx- orthopyroxene. Other abbreviations as in Table 2. Atomic proportions are calculated on 6 oxigens.

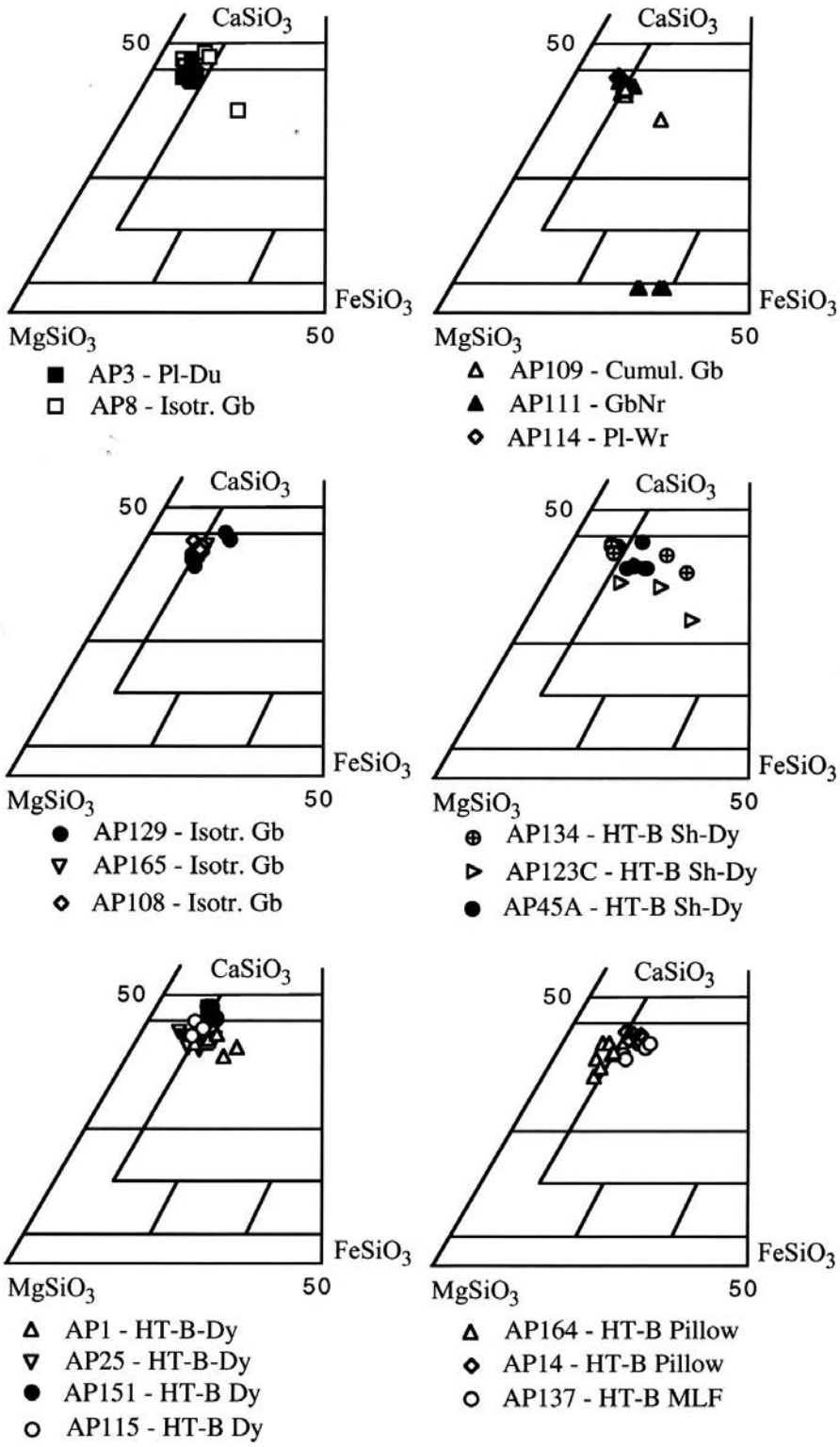

Fig. 4 - Plots of pyroxene compositions expressed in terms of Enstatite-Ferrosilite-Wollastonite for the SAM ophiolites. Pl-Du- plagioclase dunite; Sh-Dy- sheeted dykes; MLF- massive lava flow Other abbreviations as in Fig. 3.

2.29wt%), and are found as both anhedral and skeletal small-grained crystals in gabbros, and euhedral crystals in the groundmass of volcanic rocks. All analyzed Fe-Ti oxides exhibit low Cr_2O_3 content (<0.03wt%).

WHOLE-ROCK CHEMISTRY

All the rocks studied in this paper have experienced variable extents by ocean-floor metamorphism. This metamorphism may have potentially modified the whole-rock compositions; consequently, the following discussion will mainly focus on those elements whose abundances are considered relatively unmodified by the metamorphic effects. In general, these elements are Ti, P, V, Y, Zr, and REE.

Intrusive sequence

The ultramafic cumulates range in composition from plagioclase-dunites to plagioclase-wehrlites, depending on the modal amount of clinopyroxene; i.e., on the amount of trapped intercumulus liquid and this is reflected in their bulk-rock composition (Table 5). The cumulate textures are preserved, and are characterized by olivine and, occasional-

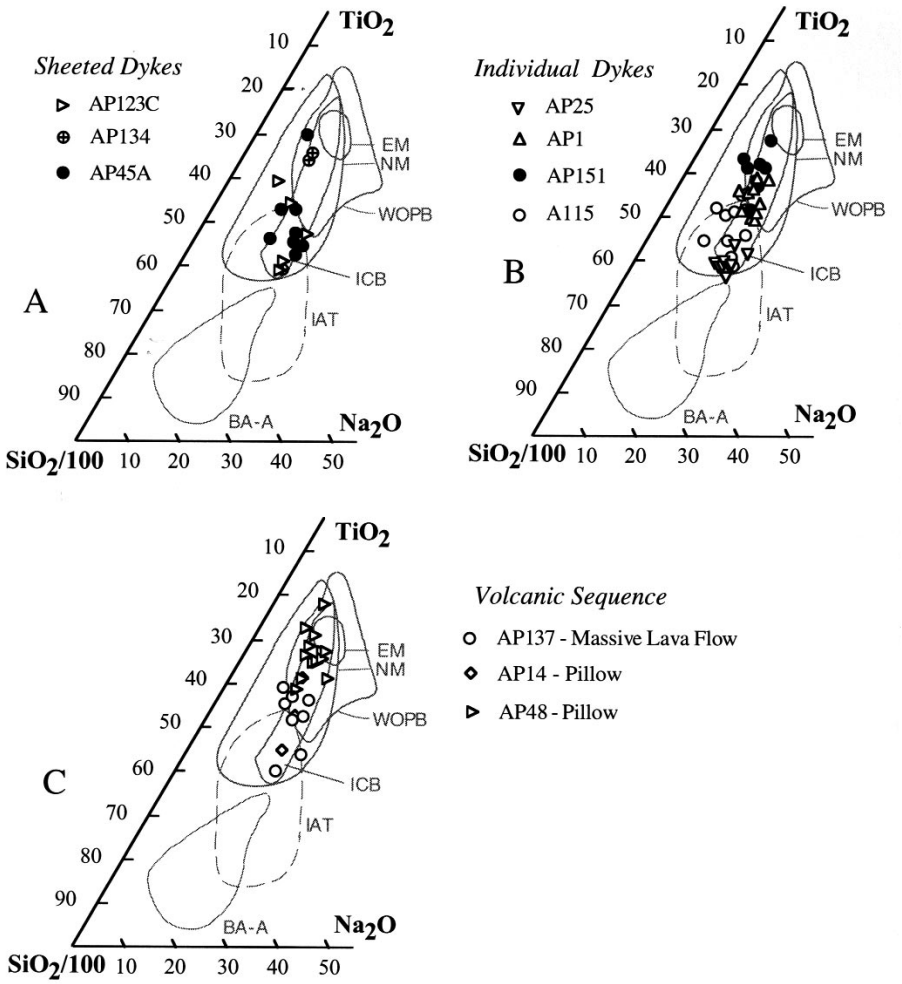

Fig. 5 - $SiO_2/100$-Na_2O-TiO_2 discriminant diagram for clinopyroxenes from the SAM ophiolitic basaltic rocks. NM- normal MORB; EM- enriched MORB; ICB- Iceland basalts; IAT- island-arc tholeiites; WOPB- within-plate ocean basalts; BA-A- intraoceanic fore-arc basalts and basaltic andesites.

Table 4 - Selected microprobe analyses of chrome spinel and Fe-Ti oxides from the SAM ophiolites.

	Intrusive Sequence						Sheeted Dykes		Volcanic and Subvolcanic Sequence			
Locality	Marcului	Sovarului	Sovarului	Julita	Almasel	A-Saliste	Julita	Julita	Sovarului	Sovarului	Batuta	Zam
Sample	AP114	AP3	AP3	AP129	AP165	AP8	AP45A	AP45A	AP1	AP1	AP137	AP13
Rock	Pl-Wr	Pl-Du	Pl-Du	Gb	Gb	Gb	HT-B	HT-B	HT-B	HT-B	HT-B	HT-B
Note									Dyke	Dyke	MLF	MLF
Mineral	CrSp4-1	Sp2-1	Sp2-2	Mt3-1	Ti-Mt3-1	Mt3-1	TiMt1-1	TiMt2-2	Mt3-1	TiMt3-2	Mt1-2	MtL-1
TiO_2	2.54	0.46	0.62	0.00	11.64	0.30	24.31	10.16	1.81	15.98	0.04	0.09
Al_2O_3	15.30	9.53	8.55	0.00	0.38	0.31	0.88	0.18	0.14	0.97	0.12	1.24
Cr_2O_3	36.86	55.89	54.19	0.03	0.00	0.11	0.00	0.03	0.00	0.03	0.00	0.00
Fe_2O_3	0.00	0.00	0.00	0.00	0.00	0.00	0.00	0.00	0.00	0.00	0.00	0.00
FeO	35.54	23.15	28.39	79.88	81.00	91.47	66.42	81.17	87.90	74.81	77.34	83.43
MnO	0.19	0.03	0.00	0.00	0.00	0.01	0.55	0.66	0.12	1.74	0.00	0.00
MgO	7.89	10.36	7.17	0.18	0.06	0.00	0.55	0.03	0.12	0.00	0.28	0.46
Oxide total	98.32	99.42	98.92	80.09	93.08	92.20	92.71	92.23	90.09	93.53	77.78	85.22
Fe_2O_3*	12.61	5.69	6.23	59.41	44.38	67.17	17.50	47.03	62.88	34.92	57.55	61.65
FeO*	24.20	18.03	22.78	26.42	41.06	31.02	50.68	38.85	31.31	43.39	25.55	27.95
Total*	99.58	99.99	99.54	86.04	97.52	98.93	94.46	96.94	96.39	97.03	83.54	91.39
Ti	0.063	0.011	0.016	0.000	0.341	0.009	0.720	0.300	0.054	0.467	0.001	0.003
Al	0.596	0.372	0.344	0.000	0.017	0.014	0.041	0.008	0.007	0.044	0.007	0.061
Cr	0.964	1.463	1.464	0.001	0.000	0.003	0.000	0.001	0.000	0.001	0.000	0.000
Fe^{3+}	0.314	0.142	0.160	1.999	1.301	1.965	0.519	1.390	1.885	1.021	1.991	1.933
Fe^{2+}	0.669	0.499	0.651	0.988	1.337	1.008	1.670	1.276	1.043	1.410	0.982	0.974
Mn	0.005	0.001	0.000	0.000	0.000	0.000	0.018	0.022	0.004	0.057	0.000	0.000
Mg	0.389	0.511	0.365	0.012	0.003	0.000	0.032	0.002	0.007	0.000	0.019	0.029
Cation total	3.000	3.000	3.000	3.000	3.000	3.000	3.000	3.000	3.000	3.000	3.000	3.000
Mg#	36.8	50.6	35.9	1.2	0.3	0.0	1.9	0.1	0.7	0.0	1.9	2.9
Cr#	61.8	79.7	81.0	100.0	0.0	19.2	0.0	10.1	0.0	2.0	0.0	0.0
Ulvospinel	6.3	1.2	1.6	0.0	34.1	0.9	72.0	30.0	5.4	46.7	0.1	0.3
Spinel	29.8	18.6	17.2	0.0	0.9	0.7	2.0	0.4	0.3	2.2	0.3	3.1
Chromite	48.2	73.2	73.2	0.1	0.0	0.2	0.0	0.1	0.0	0.1	0.0	0.0
Magnetite	15.7	7.1	8.0	100.0	65.0	98.2	25.9	69.5	94.3	51.1	99.5	96.7

CrSp- chrome spinel; Sp- spinel; Mt- magnetite; TiMt- titaniferous magnetite; Cr#- 100*Cr/(Cr+Al). Other abbreviations as in Tables 2 and 3. Atomic proportions are calculated on 4 oxigens.

Table 5 - Representative major and trace element data for selected samples from the SAM ophiolites.

	Intrusive Sequence										Sheeted Dyke Complex					
Locality	Sovarului	Marcului	A.Saliste	A.Saliste	V.Rosiuta	V.Rosiuta	Julita	Cuias	Ciungani	Ciungani	Julita	Julita	Julita	Julita	Lalasint	Ampoita
Sample	AP 3	AP114	AP 8	AP 11	AP109	AP111	AP125	AP177	AP179	AP182	AP 45A	AP123A	AP123B	AP123C	AP133B	565
Rock	Pl-Du	Pl-Wr	Gb	Di	Gb	GbNr	Gb	Gb	Fe-Gb	Fe-Gb	HT-B	HT-B	HT-A	HT-B	HT-B	HT-B
Note			Isotr.	Isotr.	Cum.	Cum.	Isotr.	Isotr.	Cum.	Cum.						
SiO_2	39.22	41.77	54.97	53.71	48.87	47.71	49.38	48.26	41.67	41.74	48.11	51.55	57.64	48.11	49.54	55.62
TiO_2	0.27	0.47	0.44	1.48	1.00	0.95	0.62	1.07	3.12	2.85	1.53	2.52	1.72	1.25	2.23	2.00
Al_2O_3	4.74	7.02	13.22	20.20	17.61	16.18	17.65	15.13	15.06	16.22	16.37	12.36	12.91	17.84	13.43	13.95
Fe_2O_3	1.31	0.00	0.78	0.41	0.99	1.07	1.04	1.27	2.04	1.97	1.46	1.72	1.59	1.33	1.66	1.38
FeO	8.74	11.53	5.21	2.76	6.60	7.13	6.93	8.50	13.63	13.13	9.73	11.48	10.60	8.88	11.05	9.17
MnO	0.15	0.18	0.16	0.06	0.14	0.12	0.13	0.14	0.20	0.20	0.17	0.16	0.11	0.16	0.15	0.16
MgO	32.98	30.04	8.78	4.40	8.22	12.95	9.47	10.24	8.65	7.92	7.01	5.77	2.78	7.33	6.87	5.82
CaO	2.19	4.06	11.70	9.16	9.53	9.51	12.67	11.62	12.80	12.81	11.01	8.34	4.72	11.03	9.62	4.25
Na_2O	0.00	0.36	2.45	4.93	3.47	1.66	1.81	1.62	1.76	1.70	2.58	4.47	6.24	2.39	3.34	5.19
K_2O	0.02	0.07	0.92	0.60	0.80	0.13	0.05	0.06	0.13	0.18	0.25	0.21	0.02	0.25	0.08	0.10
P_2O_5	0.01	0.04	0.18	0.59	0.21	0.18	0.11	0.09	0.09	0.09	0.27	0.34	0.92	0.24	0.23	0.31
LOI	10.37	4.44	1.19	1.69	2.57	2.41	0.13	2.01	0.85	1.19	1.49	1.08	0.75	1.19	1.81	2.05
Tot	100.00	100.00	100.00	100.00	100.00	100.00	100.00	100.00	100.00	100.00	100.00	100.00	100.00	100.00	100.00	100.00
CO_2																
Mg#	87.1	84.1	75.0	74.0	68.9	76.4	70.9	68.2	53.1	51.8	56.2	47.3	31.9	59.5	52.6	53.1
Zn	72	80	49	24	50	63	50	30	83	117	93	41	29	87	37	79
Ni	1438	1010	94	31	46	250	135	63	13	18	81	25	7	92	37	7
Co	110	106	23	8	31	47	39	46	58	57	43	37	25	40	38	23
Cr	2035	2766	540	13	95	314	587	126	63	51	337	45	13	371	42	16
V	85	112	242	197	231	196	184	393	980	1069	311	487	38	256	412	251
Rb	n.d.	2	20	19	15	n.d.	2	n.d.	3	4	n.d.	n.d.	2	2	2	n.d.
Sr	8	44	300	725	272	132	108	190	220	241	129	164	47	129	162	112
Ba	29	14	235	190	263	14	10	55	20	20	50	41	17	38	38	48
Nb	n.d.	2	4	9	4	5	n.d.	3	2	3	3	9	18	5	6	7
Zr	26	43	108	99	78	72	47	32	20	34	121	191	355	102	165	217
Y	9	13	27	39	26	23	20	21	16	14	37	55	104	38	51	57

	Volcanic Sequence												Dolerite Dykes			
Locality	Toc	Toc	Zam	Temesesti	Ponor	Varadia	Lalasint	Batuta	Tataroaia	Cazanesti	Podeni	V.Rosiuta	Julita	Sovarului	Ponor	V.Rachis
Sample	AP 48	AP141	AP 13	AP 40	AP 24	AP 46	AP135	AP136	AP164	AP172	AP149	AP112	AP130	AP 1	AP 25	AP151
Rock	HT-B	HT-B	HT-BA	HT-B	HT-B	HT-BA	HT-B	HT-B	HT-B	HT-B	HT-B	HT-B	HT-B	HT-B	HT-B	HT-B
Note	Pillow	MLF	MLF	Pillow	Pillow	MLF	Pillow	MLF	Pillow	Pillow	Pillow	Pillow				
SiO_2	39.12	48.01	53.04	45.66	47.11	53.14	47.49	47.64	48.27	50.13	46.58	48.70	48.73	46.93	47.28	47.84
TiO_2	0.92	1.05	1.84	1.49	1.00	2.05	2.63	1.82	0.89	2.01	1.08	1.46	1.44	1.65	0.86	1.25
Al_2O_3	14.79	15.24	14.44	16.19	13.79	13.34	13.91	15.72	16.76	14.39	17.08	15.54	16.00	14.58	15.46	14.80
Fe_2O_3	0.98	1.29	1.38	1.21	1.19	1.57	1.78	1.55	1.25	1.59	1.06	1.28	1.39	1.39	1.09	0.84
FeO	6.55	8.60	9.21	8.04	7.95	10.49	11.86	10.34	8.37	10.59	7.04	8.56	9.26	9.27	7.27	5.58
MnO	0.17	0.20	0.16	0.18	0.15	0.20	0.16	0.19	0.16	0.16	0.14	0.16	0.16	0.21	0.12	0.09
MgO	6.71	10.14	4.75	6.40	10.18	6.08	7.25	7.61	9.24	7.38	8.48	9.95	7.93	7.55	9.38	4.52
CaO	18.14	11.49	5.16	11.58	9.44	6.73	8.88	10.24	11.01	7.40	9.79	7.11	9.83	11.63	11.77	13.36
Na_2O	2.07	2.23	6.39	3.58	3.45	5.21	2.38	2.63	2.61	3.55	3.95	3.91	2.41	1.71	2.52	5.19
K_2O	0.53	0.05	0.60	0.96	0.16	0.10	0.17	0.29	0.12	0.07	0.53	0.31	0.08	0.05	0.20	0.79
P_2O_5	0.17	0.16	0.18	0.26	0.12	0.42	0.32	0.29	0.15	0.24	0.13	0.21	0.24	0.24	0.11	0.20
LOI	9.83	1.55	2.84	4.46	5.46	0.66	3.17	1.68	1.17	2.49	4.13	2.80	2.52	4.80	3.93	5.53
Tot	100.00	100.00	100.00	100.00	100.00	100.00	100.00	100.00	100.00	100.00	100.00	100.00	100.00	100.00	100.00	100.00
CO_2	7.11			2.17	2.85			0.22			0.82					4.36
Mg#	64.6	67.7	47.9	58.6	69.5	50.8	52.1	56.7	66.3	55.4	68.2	67.4	60.4	59.2	69.7	59.1
Zn	60	73	77	81	46	79	134	109	77	100	84	79	63	82	34	67
Ni	127	96	15	140	55	31	38	79	60	31	247	129	65	55	74	66
Co	40	44	27	41	40	32	46	43	45	40	54	42	37	43	41	21
Cr	302	346	30	354	129	85	61	270	195	37	413	336	170	107	180	275
V	193	281	445	269	287	299	445	347	256	390	195	282	302	331	255	220
Rb	3	2	6	32	3	2	n.d.	3	2	n.d.	8	7	n.d.		3	18
Sr	213	115	114	210	172	70	120	170	107	147	294	222	144	167	187	312
Ba	79	18	79	108	52	27	23	44	23	38	105	56	54	94	69	146
Nb	2	3	6	7	3	12	8	5	n.d.	5	n.d.	7	6	4	2	n.d.
Zr	66	77	129	136	69	337	247	137	50	174	76	111	115	117	56	85
Y	25	32	38	34	32	77	68	44	30	53	24	33	41	35	23	27

Fe-Gb- ferrogabbro; HT- high-Ti; B- basalt; BA- basaltic andesite; A- andesite; Isotr.- isotropic texture; Cum.- cumulitic texture. Oother abbreviations as in Tables 2 and 3.

ly, plagioclase and spinel as cumulus phases, whereas poikilitic pyroxenes are the intercumulus minerals. As a consequence, the crystallization order appears to be: (Cr-spinel) + olivine → plagioclase, clinopyroxene → orthopyroxene, i.e., the typical MORB sequence. The ultramafic cumulates display an extremely refractory character, having Mg# greater than 84. Nonetheless, Al_2O_3 and CaO are fairly abundant (Table 5), depending on the modal plagioclase and pyroxene content.

Mafic intrusive rocks include olivine-gabbros, gabbros, leucogabbros, Fe-gabbros, and quartz-diorites; scarce gabbronorites are also present, all showing a clear High-Ti magmatic affinity. In particular, TiO_2 content in gabbros ranges from 0.14 wt% to 2.58 wt%, while in Fe-gabbros it ranges from 2.85wt% to 3.12wt% (Table 5). The overall geochemical characteristics (Table 5) display a wide range of variation, depending on the cumulitic vs. isotropic nature of these mafic intrusives, as well as their wide degrees of fractionation (Mg# = 85-64 in gabbros and 53-51 in Fe-gabbros). HFSE concentrations are variable, in both cumulate and isotropic rocks. Nb, Zr, and Y have ranges of 2-9 ppm, 7-195 ppm, and 6-78 ppm, respectively. Within a single intrusive body, whole-rock abundances of both major and trace elements do not vary systematically with stratigraphic height, possibly supporting the hypothesis of fractionation in an open system. In addition, no systematic geochemical differences between samples from different gabbroic bodies are found, suggesting common chemical features of the parental magmas.

The plot of $FeO_t/(MgO+FeO_t)$ vs. TiO_2 diagram (Fig. 6) has been utilized for gabbroic rocks to distinguish between high-Ti and low-Ti gabbros (Serri, 1981). All analyzed samples plot in the High-Ti ophiolite field.

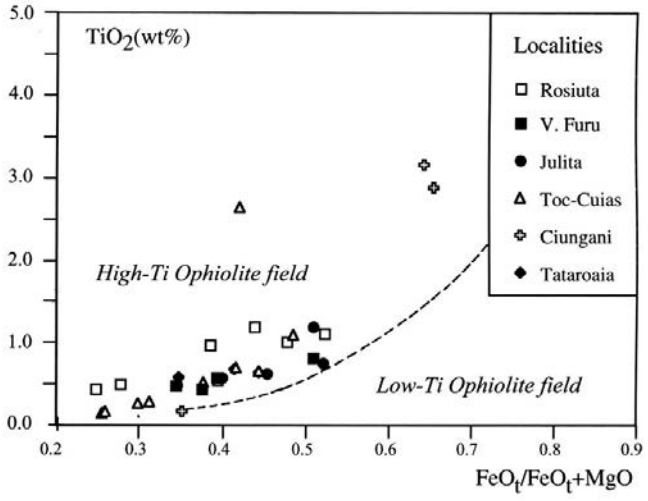

Fig. 6 - FeO_t/FeO_t +MgO vs. TiO_2 discriminant diagram for gabbroic rocks from the SAM ophiolites. Modified after Serri (1981).

Sheeted Dyke Complex

The sheeted dyke complex is formed by basaltic and subordinate basaltic-andesitic dykes. Dykes reveal different textures, ranging from fine- to medium-grained aphyric to plagioclase porphyritic types with intergranular to doleritic textures and one-way chills. A clear high-Ti magmatic affinity is evident on the Ti/V discrimination diagram (Fig. 7), as well as on Fig. 8a, where the incompatible element concentrations are shown. The diagram of Fig. 7 also shows

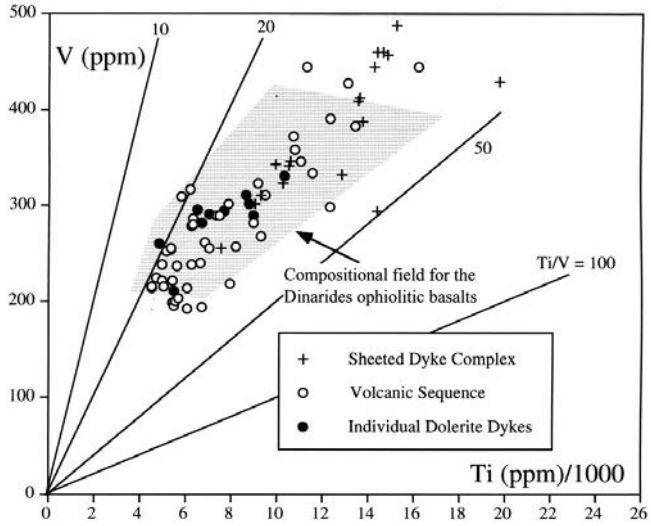

Fig. 7 - Ti (ppm)/1000 vs. V (ppm) diagram (modified after Shervais, 1982) for mafic volcanic and subvolcanic rocks from the SAM ophiolites. Shaded fields indicate the composition of Dinarides ophiolitic volcanic and subvolcanic rocks (data from Trubelja et al., 1995).

that the dykes have higher Ti/V ratios than the overlying pillow lavas and are therefore the product of higher degrees of fractionation. This conclusion is also confirmed by the Mg# (60.8 - 31.0) and by by high contents of HFSE (Fig. 8a). Compatible element amounts (Table 5) also suggest that some of these rocks derived from moderately to highly differentiated magmas.

The major and trace element covariations for the analyzed dykes, shown in Fig. 9, also confirm this conclusion. The increase of TiO_2, FeO_t, V with decreasing Mg# (up to about 42) followed by a strong decrease of these elements indicate that the magmas become sufficiently evolved that minor phase crystallization take place. Chondrite-normalized rare earth elements (REE) patterns range from moderately light REE (LREE) depleted to almost flat patterns (Fig. 10), as also shown by the La_N/Sm_N ratios (0.75-0.99).

Volcanic Sequence and Individual Dolerite Dykes

The volcanic sequence is by far the most abundant part of the ophiolitic sequence, and is predominantly composed of basalts and basaltic andesites (Table 5). Basaltic rocks show a wide range of geochemical compositions (Table 5). Though the chemistry of volcanic rocks largely overlaps with that of the sheeted dykes, it shows a relatively lower degree of fractionation (Mg# = 70-40), as well as lower contents in HFSE (Fig. 8b, c, d). Like the dykes, the high-Ti (MORB) geochemical affinity of the pillow lavas is clearly indicated by the TiO_2 content (0.73-2.98wt%), P_2O_5 (0.13-0.42wt%), Y (20-68ppm) and Ti/V ratios (20-40, Fig. 7). Similarly, the Fe-enrichment trend and the flat N-MORB-normalized HFSE pattern (Fig. 8b, c, d) are consistent with a N-MORB composition. The strong enrichment in low field strength elements (LFSE) shown by the Rimetea nappe samples (Table 5) is due to the high degree of alteration generally observed in all the Rimetea nappe magmatic associations. Chondrite-normalized REE patterns (Fig. 10) are almost flat (La_N/Sm_N ratios = 0.83-0.91).at 10 to 50 times chondritic abundance, these pattern which seems to be intermediate between modern N-MORB and T-MORB (e.g. Sun et al., 1979). Slight negative Eu anom-

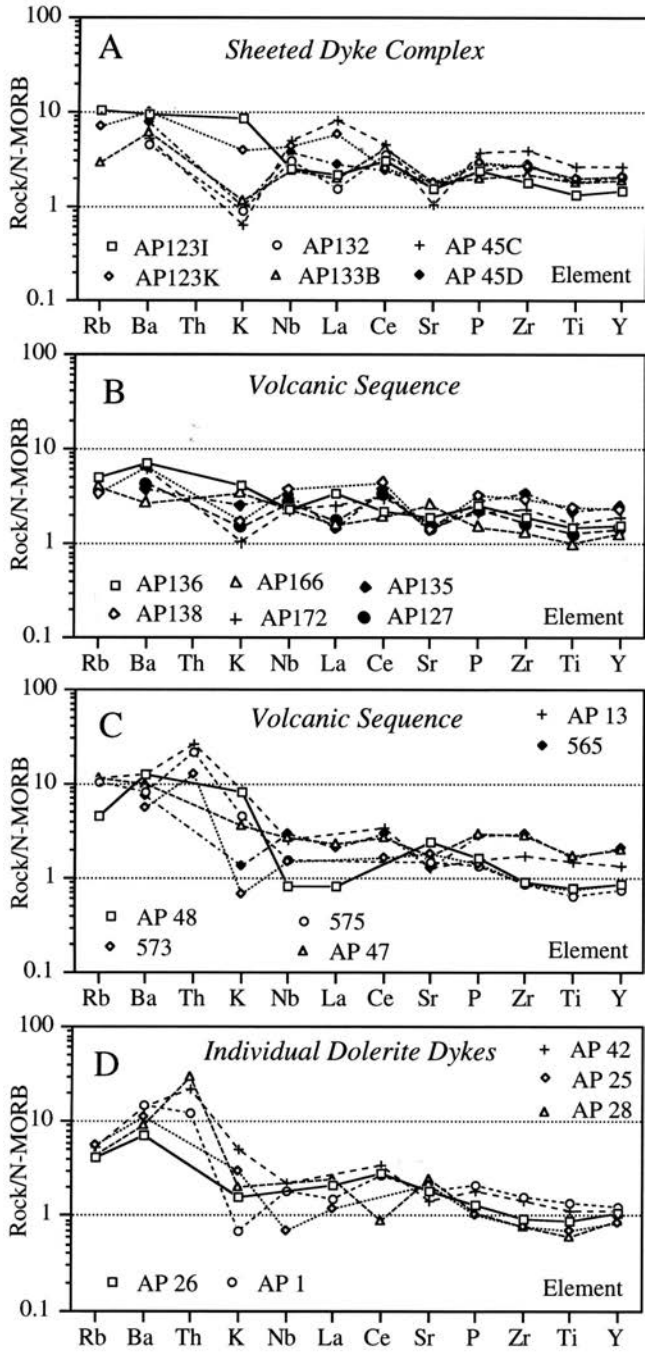

Fig. 8 - Rock/N-MORB incompatible element diagrams for mafic volcanic and subvolcanic rocks from the SAM ophiolites. Normalizing values are from Sun and McDonough (1989).

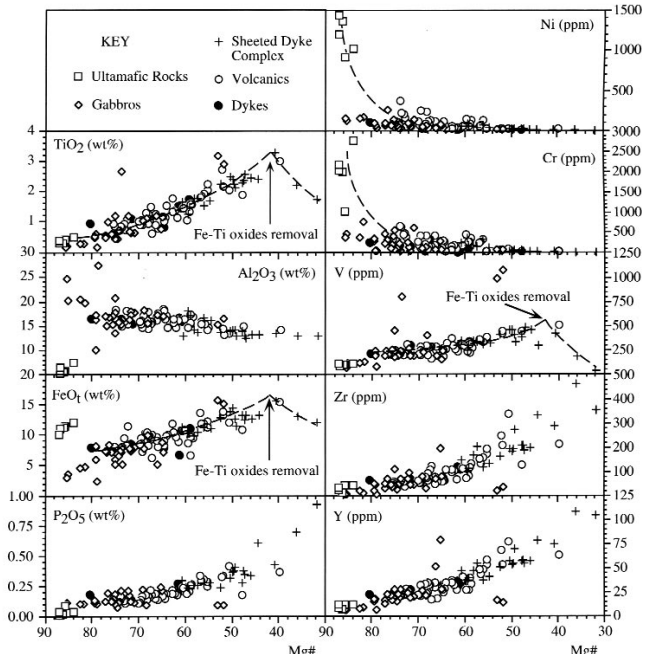

Fig. 9 - Selected major and trace elements vs. Mg# variation diagrams for the SAM ophiolitic rocks.

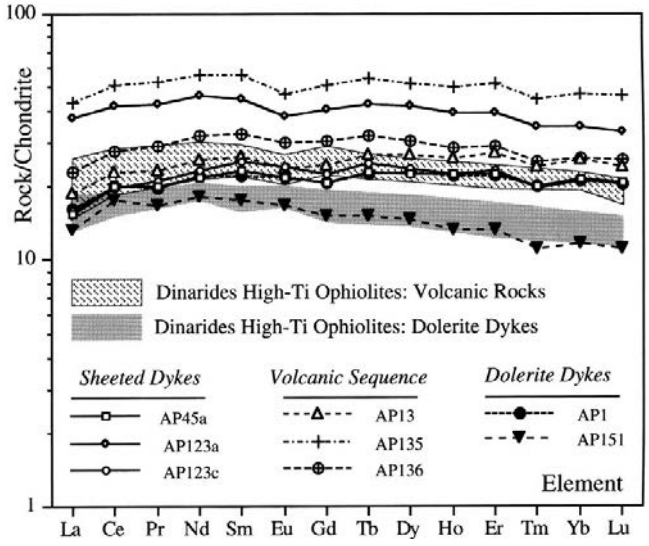

Fig. 10 - Chondrite-normalized REE patterns for selected mafic volcanic and subvolcanic rocks from the SAM ophiolites. Normalizing values are from Sun and McDonough (1989). Fields for Dinarides ophiolitic volcanic and subvolcanic rocks are reported for comparison (data from Trubelja et al., 1995).

alies in the more evolved magmas reflect the early crystallization of plagioclase.

The individual dolerite dykes are compositionally similar to the mafic volcanic rocks (Tables 5 and 6). This similarity is also expressed in the REE plots (Fig. 10) and the diagrams of Figs.9, 10, and 11. Nonetheless, some dolerite dykes show a weak enrichment in LREE compared to HREE (e.g. sample AP151 in Fig. 10), which account for a possible T-MORB character of these rocks, suggesting likely differences in the mantle source which contributed to the upper crust rocks.

DISCUSSION

Geochemical variations and evolutionary trend of SAM ophiolites

Variations in selected major and trace element abundances are illustrated in Fig. 9. SAM ophiolites exhibit a single fractionation trend, clearly indicating a cogenetic origin. In subvolcanic and volcanic rocks, TiO_2, V, and to a lesser extent FeO_t, increase of concentration up to ca. 40 Mg#, after which this a sudden decrease is observed. The decrease of these elements is related to the extensive crystallization of Ti- and Fe-bearing phases in their intrusive counterparts, i.e., the Fe-gabbros (Fig. 9). Al_2O_3 is charac-

Table 6 - ICP-MS analyses for selected samples from the SAM ophiolites.

Locality	Julita	Julita	Julita	Zam	Lalasint	Batuta	Sovarul.	V.Rachis
Sample	AP 45A	AP123A	AP123C	AP 13	AP135	AP136	AP 1	AP151
Rock	HT-B	HT-B	HT-B	HT-BA	HT-B	HT-B	HT-B	HT-B
Note	Sh-Dy	Sh-Dy	Sh-Dy	MLF	Pillow	MLF	Dyke	Dyke
Sc	92.4	93.5	99.1	81.1	111	105	88.7	76.5
Nb	2.97	6.94	2.71	2.91	7.63	4.03	3.37	1.33
Hf	3.01	3.80	2.72	3.75	7.92	3.39	2.96	2.09
Ta	0.26	0.62	0.23	0.36	0.62	0.35	0.94	0.36
Th	0.19	0.66	0.16	0.55	0.68	0.25	0.23	0.32
U	0.08	0.19	0.06	0.34	0.31	0.09	0.08	0.33
La	3.62	8.94	3.78	4.45	10.3	5.41	3.85	3.17
Ce	12.2	25.9	12.1	13.9	31.5	17.0	12.2	10.8
Pr	1.89	4.10	1.99	2.21	5.03	2.75	1.87	1.59
Nd	10.2	21.6	10.8	11.9	26.5	14.9	10.2	8.39
Sm	3.53	6.84	3.81	4.00	8.63	4.94	3.36	2.69
Eu	1.24	2.23	1.37	1.36	2.74	1.73	1.25	0.97
Gd	4.25	8.40	4.59	4.97	10.5	6.24	4.23	3.09
Tb	0.85	1.61	0.92	1.00	2.05	1.20	0.83	0.57
Dy	5.71	10.7	5.98	6.77	13.2	7.69	5.78	3.72
Ho	1.26	2.22	1.27	1.47	2.83	1.61	1.25	0.75
Er	3.71	6.51	3.80	4.46	8.59	4.77	3.64	2.19
Tm	0.50	0.88	0.50	0.60	1.15	0.64	0.51	0.28
Yb	3.59	5.92	3.53	4.29	8.00	4.41	3.55	1.99
Lu	0.52	0.83	0.52	0.60	1.17	0.65	0.52	0.28

HT- high-Ti; B- basalt; BA- basaltic andesite; Sh-Dy- sheeted dykes; MLF- massive lava flow.

terized by a smooth decrease of concentrations with decreasing Mg#, coupled with highly variable concentrations in cumulate rocks, presumably depending on the cumulation of plagioclase. P_2O_5, Zr, Y, and the HFSE, increase with decreasing Mg#. A sharp increase of the slopes are observed for Mg# < 60, as a consequence of the onset of apatite and zircon crystallization in the respective magmas. Cr and Ni identify a typical, decrease with decreasing Mg#. In Fig. 9, it is also apparent that the compositions of individual dolerite dykes are largely overlapped over those of volcanics. By contrast, sheeted dyke samples represent liquids generally more evolved than those of the volcanic sequence. In summary, the evolutionary trend of the SAM ophiolite magmatic rocks (Fig. 9) is characterized by early removal and accumulation in the ultramafic cumulates of chrome spinels and olivine followed by the removal and accumulation of plagioclase and pyroxenes in gabbros and, eventually, Ti- and Fe-bearing phases. The major and trace element variations observed along the fractionation trend are similar to those described either in present-day MORBs, or in high-Ti ophiolites from the circum-Mediterranean belts, and best compare with the magmatic evolution occurring in the open systems below mid-ocean ridges.

Tectono-magmatic setting of SAM ophiolites

One of the purposes of this paper is to improve the characterization of the tectonic environment in which SAM ophiolites originated. As noted earlier; different interpretations have been provided. They span from mid-ocean ridge (Savu, 1990; 1996; Savu et al., 1981; 1994b) to island arc (Cioflica et al., 1980; Cioflica et al., 1981; Nicolae et al., 1992) and marginal basin (Cioflica and Nicolae, 1981; Nicolae, 1985) settings. In addition, some authors consider the ophiolitic sequence and the overlying calc-alkaline series as genetically related (Cioflica and Nicolae, 1981; Nicolae et al., 1992).

A variety of discriminant diagrams have been devised for distinguishing between the different volcanic rock types from ophiolitic complexes and their bearing on the possible tectonic environments of formation (e.g., Pearce and Cann, 1973; Pearce and Norry, 1979; Beccaluva et al., 1989; Shervais, 1982; and many others). The $FeO_t/(MgO+FeO_t)$ and TiO_2 petrogenetic parameters of ophiolitic gabbroic rocks have been utilized by Serri (1981) to distinguish between complexes originating at mid-ocean ridge and supra-subduction basins, labeled high-Ti and low-Ti respectively. Pearce et al. (1984) have classified ophiolitic complexes as MORB-type and supra-subduction zone (SSZ) type. High-Ti (MORB) ophiolites include a number of Tethyan ophiolitic complexes, from the Northern Apennines and Corsica (Beccaluva et al., 1983), as well as from the Alps and the High-Ti Dinaride-Albanide-Hellenide (Beccaluva et al., 1984; 1994) ophiolitic complexes. These are characterized by basalts which are geochemically similar to normal MORBs, a MORB-like crystallization sequence of olivine → plagioclase → Ca-rich pyroxene, and a very restricted occurrence (or even absence) of rock types such as diorite and plagiogranite. Low-Ti (SSZ) ophiolites, such as the low-Ti Dinaride-Albanide-Hellenide ophiolitic complexes (Beccaluva et al., 1984; 1994; Bébien et al., 1987) contain lavas with volcanic-arc affinities (including boninites); they show a crystallization sequence of olivine → pyroxenes → plagioclase, and abundant plagiogranites and sheeted dykes.

In this paper we have considered the mineral chemistry and whole-rock chemistry of both intrusive and volcanic rocks from the SAM ophiolites, together with petrographical and geological observations. Fig. 6 shows a plot of $FeO_t/(MgO+FeO_t)$ vs. TiO_2 for the gabbroic rocks. The SAM data plot in the high-Ti field, defining a trend very similar to that of the abyssal gabbros. The MOR environment is fully shown in Fig. 7, where all SAM ophiolitic basalts plot within the field for MORBs ($20<Ti/V<50$). From Fig. 7 it is also apparent that the studied rocks display quite uniform Ti/V ratios, suggesting that the possible primary melts were generated from mantle sources sharing similar geochemical features (Shervais, 1982). Another petrogenetic discriminant that has been proposed as an indicator of tectonic environment is the compositional variation of clinopyroxene in basaltic rocks (Beccaluva et al., 1989). Fig. 5 shows the compositions of clinopyroxene from SAM ophiolitic basalts. These data, in agreement with the previous ones, indicate that the clinopyroxenes originate in a mid-ocean ridge environment.

In addition, the crystallisation order - and, consequently, the succession of lithologies - is similar to that of the high-Ti ophiolitic series (Beccaluva et al., 1984). Finally, the abundance of trace elements (Figs. 8, 9) and the REE patterns (Fig. 10) suggest that the compositional characteristics of these volcanics are similar to those of typical MORB tholeiites. There is therefore no evidence for an island-arc related setting of the SAM ophiolites, as proposed by previous authors (Cioflica et al., 1980; Cioflica and Nicolae, 1981; Nicolae, 1995).

Burchfiel (1980) suggested that the present-day location of the SAM ophiolites in the internal side of the Carpathian belt is probably the consequence of a dextral transpression of about 300 km along the south-Transylvanian Miocenic fault-system. Therefore, the pre-Miocenic position of SAM ophiolites should be located in the northward prolongation of the Dinarides ophiolites. As a consequence, a petrogenetic connection between SAM and Dinarides ophiolites can reasonably be postulated. Geological evidence supporting this hypothesis is scarce because the SAM ophiolites are highly dismembered. Nonetheless, many petrochemical features of the SAM ophiolites can be recognized in the MOR-

type ophiolites of the Hellenic-Dinaric belt (Lugovic et al., 1991; Trubelja et al., 1995). In addition, the association of SAM ophiolites with the Late Jurassic island arc magmatic series and related granitoid intrusions outline a similarity with the ophiolites from the Hellenic-Dinaric Vardar Zone (Bébien et al., 1987), where MOR basaltic rocks are associated with island arc tholeiitic volcanics and calc-alkaline granites of Late Jurassic age. Chemical similarities between SAM and Dinarides ophiolites can be seen in the Ti-V diagram (Fig. 7). Further evidence of these chemical analogies is given by the REE contents. In particular, while volcanic rocks from the Dinarides ophiolites display a depletion in LREE in comparison with HREE, most of the dolerite dykes are characterized by a weak enrichment in LREE compared to HREE (Trubelja et al., 1995). Very similar trends are observed in the SAM ophiolites (Fig. 10).

CONCLUSIONS

Suggestions that the ophiolitic rocks from the SAM were formed at a mid-ocean ridge spreading centre are supported by:

1- the MORB-like crystallization of (chrome spinel) + olivine → plagioclase → clinopyroxene → orthopyroxene (+ Fe-Ti oxides), as observed in both intrusive and volcanic rocks;

2- whole-rock major and trace element data from dolerite dykes and basalts are geochemically very similar to present-day mid-ocean ridge basalts;

3- the major and trace element covariations for the analyzed volcanic and subvolcanic rocks are consistent with the MORB fractionation trend typically occurring in a open system shallow magma chamber.

4- HFSE concentrations normalized to the N-MORB (Sun and McDonough, 1989) display typically flat patterns.

5- REE concentrations, which typically range from 10 to 50 times chondrite, and are characterized by slightly LREE depleted to almost flat chondrite-normalized patterns (La_N/Sm_N = 0.75-0.99), and a moderate HREE depletion with respect to medium-REE (Sm_N/Yb_N = 1.05-1.50);

6- mineral chemistry (with particular regard to pyroxene chemistry) from gabbros, diabases and basalts, which reveals mineral compositions almost indistinguishable from those from present-day MORBs, or from high-Ti ophiolites from the circum-Mediterranean belts.

Therefore, there is no evidence to suggest formation of SAM ophiolites in either island arc or back-arc basin tectonic settings. For these reasons, previous interpretations of the SAM ophiolitic suite as originating in a supra-subduction setting should be abandoned definitively.

Finally, SAM ophiolites display petrochemical features very similar to those observed in the high-Ti ophiolites from the Dinaric belt. This further supports the hypothesis that SAM ophiolites originally constituted a northern prolongation of the Dinaric ophiolite belt, from which they were separated by the Miocene South-Transylvanian fault (Burchfiel, 1980).

Acknowledgements

This research was supported by M.U.R.S.T. COFIN 1998 and by the Geological Institute of Romania (Institutul Geologic al Romaniei). The authors are obliged to G. Principi, V. Bortolotti, M. Marroni, and L. Pandolfi for their precious help during the field work. We wish to thank F. Olmi for the analytical facilities, as well as L. Beccaluva and E. Padoa for their critical review of the manuscript. Many thanks go to the reviewers J.A. Pearce and A. Montanini.

REFERENCES

Beccaluva L., Di Girolamo P., Macciotta G. and Morra V., 1983. Magma affinities and fractionation trends in ophiolites. Ofioliti, 8 (3): 307-324.

Beccaluva L., Ohnenstetter D., Ohnenstetter M. and Paupy A., 1984. Two magmatic series with island arc affinities within the Vourinos ophiolite. Contrib. Mineral. Petrol., 85: 253-271.

Beccaluva L., Macciotta G., Piccardo G.B. and Zeda O., 1989. Clinopyroxene compositions of ophiolite basalts as petrogenetic indicator. Chem.Geol., 77: 165-182.

Beccaluva L., Coltorti M., Premti I., Saccani E., Siena F. and Zeda O., 1994. Mid-ocean ridge and supra-subduction affinities in ophiolitic belts from Albania. Special Issue "Albanian ophiolites: state of the art and perspectives" L. Beccaluva Ed. Ofioliti, 19 (1): 77-96.

Bebien J., Baroz F., Capedri S. and Venturelli G., 1987. Magmatismes basiques associés à l'overture d'un bassin marginal dans les Héllenides internes au Jurassique. Ofioliti, 12 (1): 53-70.

Bortolotti V., Marroni M., Nicolae I., Pandolfi L., Principi G. and Saccani E., 1999. Preliminary structural and petrological data on the Southern Apuseni Mountains Upper Jurassic magmatic Units (Romania). FIST, 2° Forum Italiano Sci. Terra, Bellaria, Sett. 1999, 1: 460-461.

Burchfiel B.C., 1980. Eastern European Alpine system and the Carpathian orocline as an example of collision tectonics. Tectonophysics, 63: 31-61.

Cioflica G., Lupu M., Nicolae I. and Vlad S., 1980. Alpine ophiolites of Roumania: tectonic setting, magmatism and metallogenesis. An. Ist. Géol. Géophys., 56: 79-95.

Cioflica G., Savu H., Nicolae I., Lupu M. and Vlad S., 1981. Guide to excursion A3: Alpine ophiolitic Complexes in south Carpatian and south Apuseni Mountains. 12th Congr. Carpatho-Balcan Geol. Ass., Bucharest, Romania, 80 pp.

Cioflica G. and Nicolae I., 1981. The origin, evolution and tectonic setting of the Alpine ophiolites from the South Apuseni Mountains. Rev. Roum. Géol. Géophys. Géogr., 25: 19-29.

Dallmeyer R.D., Pana D.I., Neibauer F. and Erdmer, P., 1999. Tectonothermal evolution of the Apuseni Mountains, Romania: resolution of Variscan versus Alpine events with $^{40}Ar/^{39}Ar$ ages. J. Geol., 107: 329-352.

Dal Piaz G.V., Martin, S., Villa, I.M. and Gosso, G., 1995. Late Jurassic blueschist facies pebbles from the Western Carpathians orogenic wedge and paleostructural implications for Western Tethys evolution. Tectonics, 14 (4): 874-885.

Dick H.J.B. and Bullen T., 1984. Chromian spinel as a petrogenetic indicator in abyssal and alpine-type peridotites and spatially associated lavas. Contrib. Mineral. Petrol., 86: 54-76.

Dickey J.S.Jr., Yoder H.S. Jr. and Shairer J.F., 1971. Chromium in silicate-oxide systems. Carnegie Inst. Washington Yrb., 70: 118-122.

Franzini M., Leoni L. and Saitta M., 1975. Revisione di una metodologia analitica per fluorescenza-X, basata sulla correzione completa degli effetti di matrice. Rend. S.I.M.P., 31: 635-678.

Jackson M.L., 1958. Soil chemical analysis. Prentice-Hall, 498 pp.

Kovacs S., 1982. Problems of the "Pannonian Median Massif" and the plate tectonics concept. Contribution based on the distribution of Late Paleozoic - Early Mesozoic isopic zones. Geol. Runds., 71: 617-640.

Leoni, L. and Saitta, M., 1976. X-Ray fluorescence analysis of 29 trace elements in rock and mineral standards. Rend. S.I.M.P., 32: 497-510

Lugovic B., Altherr R., Raczek I., Hofmann A. W. and Majer, V., 1991. Geochemistry of peridotites and mafic igneous rocks from the Central Dinaric Ophiolite Belt, Yugoslavia. Contrib. Mineral. Petrol., 106 (2): 201-216.

Lupu M., Antonescu E., Avram E., Dumitrica P. and Nicolae I., 1995. Comments on the age of some ophiolites from the north Drocea Mts. Rom. J. Tect. Reg. Geol., 76: 21-25.

Morimoto N., 1989. Nomenclature of pyroxenes. Canad. Mineral., 27: 143-156.

Nicolae I., 1985. Ophiolites of the Trascau Mountains (South Apuseni Mountains). An. Inst. Geol. Geofiz., 65: 143-205.

Nicolae I., 1995. Tectonic setting of the ophiolites from the South Apuseni Mountains: magmatic arc and marginal basin. Rom. J. Tect. Reg. Geol., 76: 27-38.

Nicolae I., Soroiu, M. and Bonhomme G.M., 1992. Ages K-Ar de quelques ophiolites des Monts Apuseni du sud (Roumanie) et leur signification géologique. Géol. Alpine, 68: 77-83.

Pana D.I., 1998. Petrogenesis and tectonic of the basement rocks of the Apuseni Mountains: significance for the alpine tectonics of the Carpathian-Pannonian region. PHD thesis, Univ. of Alberta (Canada), Edmonton, 356 pp.

Pearce J.A. and Cann J.R., 1973. Tectonic setting of basic volcanic rocks determined using trace element analyses. Earth Plan. Sci. Lett., 19: 290-300.

Pearce J.A. and Norry M.J., 1979. Petrogenetic implications of Ti, Zr, Y and Nb variations in volcanic rocks. Contrib. Mineral. Petrol., 69: 33-47.

Pearce J.A., Lippard S.J. and Roberts S., 1984. Characteristics and tectonic significance of supra-subduction zone ophiolites. In: I.G. Gass, S.J. Lippard and A.W. Shelton (Eds.), Ophiolites and oceanic lithosphere, Geol. Soc. London Spec. Pap., 13: 77-94.

Sandulescu M., 1984. Geotectonica Romaniei. Edit. Tehn. Bucharest, Romania, 360 pp.

Savu H., 1980. Genesis of the alpine cycle ophiolites from Romania and their associated Calc-alkaline and Alkaline volcanics. An. Ist. Geol. Geofiz., 56: 55-77.

Savu H., 1990. Remarks on the Mesozioc magmatic activity in the Trascau Mountains (Mureş Zone). Rev. Roum. Géol. Géophis. Géogr., 34: 13-24.

Savu H., 1996. A comparative study of the ophiolite obducted from two different segments of the Mureş Ocean "normal" median ridge (Romania). Rom. J. Petrol., 77: 49-60.

Savu H., Udrescu C. and Neacsu V., 1981. Geochemistry and geotectonic setting of ophiolites and island arc volcanics of the Mureş zone (Romania). Ofioliti, 6 (2-3): 269-286.

Savu H., Udrescu C., Neacsu V. and Ichim M., 1994a. Petrology and geochemistry of the effusive rocks from the ocean floor basalt complex in the Mureş Zone. Rom. J. Petrol., 76: 67-76.

Savu H., Stoian M., Tiepac I., Grabari G. and Popescu G., 1994b. Petrological significance of REE, U, Th, K, Rb, Sr, Hf and of the $^{87}Sr/^{86}Sr$ in the basaltic complex of the Mureş Zone. Rom. J. Petrol., 76: 77-84.

Savu H., Grabari G. and Stoian M., 1996. New data concerning the structure, petrology and geochemistry of the Late Kimmerian granitoid massif of Savarsin (Mureş Zone). Rom. J. Petrology, 77: 71-82.

Serri G., 1981. The petrochemistry of ophiolite gabbroic complexes: a key for the classification of ophiolites into low-Ti and high-Ti types. Earth Planet. Sci. Lett., 52: 203-212.

Shervais J. W., 1982. Ti-V plots and the petrogenesis of modern ophiolitic lavas. Earth Planet. Sci. Letters, 59: 101-118.

Sun S.S., Nesbit R.W. and Sharaskin, A.Ya., 1979. Geochemical characteristics of mid-ocean ridge basalts. Earth Planet. Sci. Lett., 44: 119-138.

Sun S.S. and McDonough W.F., 1989. Chemical and isotopic systematics of ocean basalts: Implications for mantle composition and processes. In: A.D. Saunders and M.J. Norry, (Eds.), Magmatism in the ocean oasins. Geol. Soc. London Spec. Publ., 42: 313-346.

Trubelja F., Marchig V., Burgath K. P. and Vujovic Z., 1995. Origin of the Jurassic Tethyan ophiolites in Bosnia: A geochemical approach to tectonic setting. Geol. Croatica, 48 (1): 49-66.

Received, February 16, 2001
Accepted, May 31, 2001